Asian and Pacific Coasts 2003

AN APPLICATION OF A NESTING PROCEDURE TO A HIGHLY-RESOLVED CURRENT SIMULATION IN A MANGROVE AREA

Yasuo Nihei[1], Keita Sato[2], Yasunori Aoki[3], Tsukasa Nishimura[4] and Kazuo Nadaoka[5]

To efficiently perform the numerical simulation in a R-type mangal, in which the horizontal scales of the creek and the swamp are quite different, we attempt to apply a nesting procedure to the highly resolved current simulation in the mangrove area at Fukido River of the Ishigaki Island, Okinawa, Japan. In the computation, we introduce three computational domains with the different grid resolutions. The results indicate that the numerical performance of the nesting procedure used here is confirmed for the tidal current simulation in the mangrove estuary through the comparison of the observed and computed results. It should be also found that the present numerical model can simulate complicated flow structures around the creeks.

Keywords: mangrove, numerical simulation, nesting procedure, tidal current

1. Introduction

A riverine-forest type mangrove (R-type mangal), which is observed in most mangrove forests, is composed of meandering creeks and surrounding swamps with densely vegetated mangrove trees and roots (Lugo and Snedaker, 1974). The ratio of the swamp area to the creek area appears to be typically of order 2-10 and then the horizontal scale of the swamp is quite different with that of the creek. To predict water environments and sedimentary processes in a R-type mangal, it is desirable to conduct current simulations in which the morphological feature of a R-type mangal as mentioned above are taken into consideration. For this purpose, it may be expected to employ a nesting procedure, in which the computational results in a larger-scale domain are successively

1 Lecturer, Department of Civil Engineering, Tokyo University of Science, 2641 Yamazaki, Noda-shi, Chiba 278-8510, Japan. nihei@rs.noda.tus.ac.jp
2 Ph.D student, Department of Civil Engineering, Tokyo University of Science, 2641 Yamazaki, Noda-shi, Chiba 278-8510, Japan. j7601701@ed.noda.tus.ac.jp
3 Engineer, Design & Engineering Department, Penta-Ocean Construction Co. Ltd., 2-2-8 Koraku, Bunkyo-ku, Tokyo 112-8576, Japan. Yasunori.Aoki@mail.penta-ocean.co.jp
4 Professor, Department of Civil Engineering, Tokyo University of Science, 2641 Yamazaki, Noda-shi, Chiba 278-8510, Japan. kaiyou@rs.noda.tus.ac.jp
5 Professor, Graduate School of Information Science and Engineering, Tokyo Institute of Technology, 2-12-1 O-okayama, Meguro-ku, Tokyo 152-8552, Japan. nadaoka@mei.titech.ac.jp

reflected on a smaller-scale computation. Although numerical simulations for flow fields in R-type mangals have been performed (e.g., Mazda et al., 1995), the numerical performance has not been adequately confirmed through the comparisons of computed and observed results for hydrodynamic environments in a mangrove area. Furthermore, the nesting procedure has not been applied to the current simulations in the mangrove area.

From these reasons, in the present study, we try to apply the nesting procedure to the highly resolved current simulation in Fukido River estuary section, one of typical R-type mangals, located in the north-west part in the Ishigaki Island, Okinawa, Japan. In the current simulation, we adopt three computational domains with different grid resolutions to realize the highly resolved computation around creeks.

2. Outline of A Numerical Model and Computational Condition

2.1 *Governing equations*

The governing equations in the computation are based on the 2-D Navier-Stokes equation with the drag force for densely vegetated mangrove trees and roots in the swamp. The continuity and momentum equations are given as

$$\frac{\partial \eta}{\partial t} + \frac{\partial}{\partial x}[(h+\eta)u] + \frac{\partial}{\partial y}[(h+\eta)v] = 0\,, \tag{1}$$

$$\frac{\partial u}{\partial t} + u\frac{\partial u}{\partial x} + v\frac{\partial u}{\partial y} - fv = -g\frac{\partial \eta}{\partial x} + A_H\left(\frac{\partial^2 u}{\partial x^2} + \frac{\partial^2 u}{\partial y^2}\right) - \left(\frac{C_{fb}}{h+\eta} + \frac{aC_D}{2}\right)u\sqrt{u^2+v^2}\,, \tag{2a}$$

$$\frac{\partial v}{\partial t} + u\frac{\partial v}{\partial x} + v\frac{\partial v}{\partial y} + fu = -g\frac{\partial \eta}{\partial y} + A_H\left(\frac{\partial^2 v}{\partial x^2} + \frac{\partial^2 v}{\partial y^2}\right) - \left(\frac{C_{fb}}{h+\eta} + \frac{aC_D}{2}\right)v\sqrt{u^2+v^2}\,, \tag{2b}$$

where u and v denote the depth-averaged velocity in x and y directions, respectively and η, h, f and g mean the water elevation, water depth, Coriolis parameter and the gravitational acceleration (=9.8m/s^2), respectively. It should be noted that the effects of the bottom friction and vegetation drag in Eq. (2) are separately expressed such as the computation of river flow with vegetation layer (e.g., Nadaoka and Yagi, 1998). The coefficient for the bottom friction C_{fb} is set to be $2.6*10^{-3}$ as a standard value for a river-flow computation. For the parameter of vegetation density a and drag coefficient C_D, $aC_D/2$ =1.0m^{-1} is taken only in the swamp in line with Mazda et al. (1995). The horizontal eddy viscosity A_H in Eq. (2) is represented with the Smagorinsky model,

$$A_H = (C_s\Delta)^2\left\{2\left(\frac{\partial u}{\partial x}\right)^2 + \left(\frac{\partial v}{\partial x} + \frac{\partial u}{\partial y}\right)^2 + 2\left(\frac{\partial v}{\partial y}\right)^2\right\}^{\frac{1}{2}}, \tag{3}$$

where the constant value C_s is given to be 0.10 as a standard value and Δ represents a grid

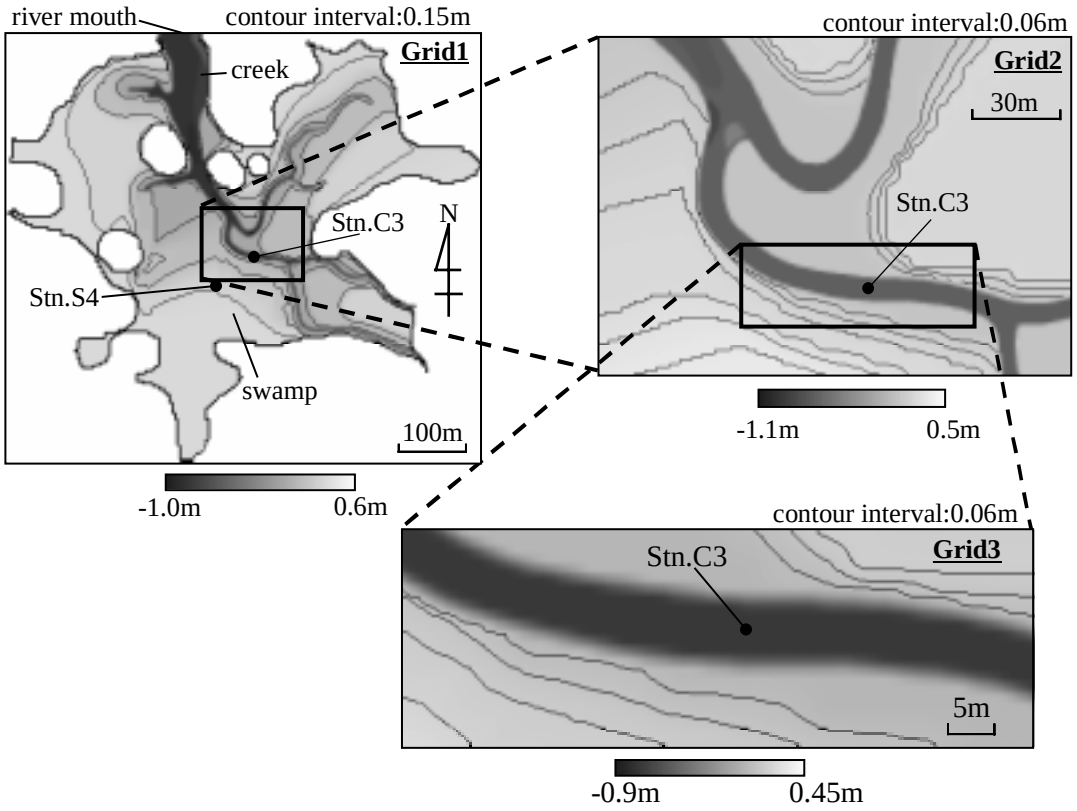

Fig. 1 Computational domains and bathymetry data.

size**.**

2.2 *Nesting grid system*

To realize the highly resolved computation for flow field in the mangrove area with computational efficiency, we introduce the three computational domains as shown in **Fig.1**. The larger-, intermediate- and smaller-scale domains, named here Grid 1, 2 and 3, have the spatial resolutions of 4m, 1m and 0.25m, respectively. Further details of the computational conditions in each domain are indicated in **Table 1**.

Since the detailed data of the bathymetry in the mangrove area is not obtained here, we do not use a new multi-nesting approach which we have recently developed for coastal ocean model to remove the difficulties in the treatment of open boundary conditions (Nihei et al., 2001). As the nesting procedure in the current simulation, therefore, we adopt a conventional one-way nesting procedure, in which the computational results in the larger-scale domain are given as the open boundary conditions for the smaller-scale computation. The ratio of the grid size in the larger-scale domain to that in the smaller-scale domain is 4 as represented in **Table 1**.

2.3 *Computational conditions*

For comparison of the computed results with observed data obtained by the authors (e.g., Nihei et

Table 1 Computational conditions in each domain.

	Grid1	Grid2	Grid3
Domain size	688×612m	144×100m	69×24m
Grid number	172×153	144×100	276×96
Grid size	4.0m	1.0m	0.25m

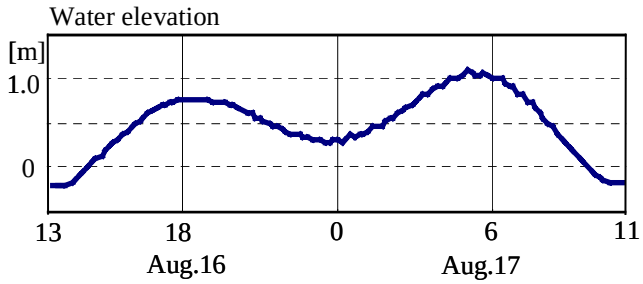

Fig. 2 Observed data for the water elevation at the river mouth.

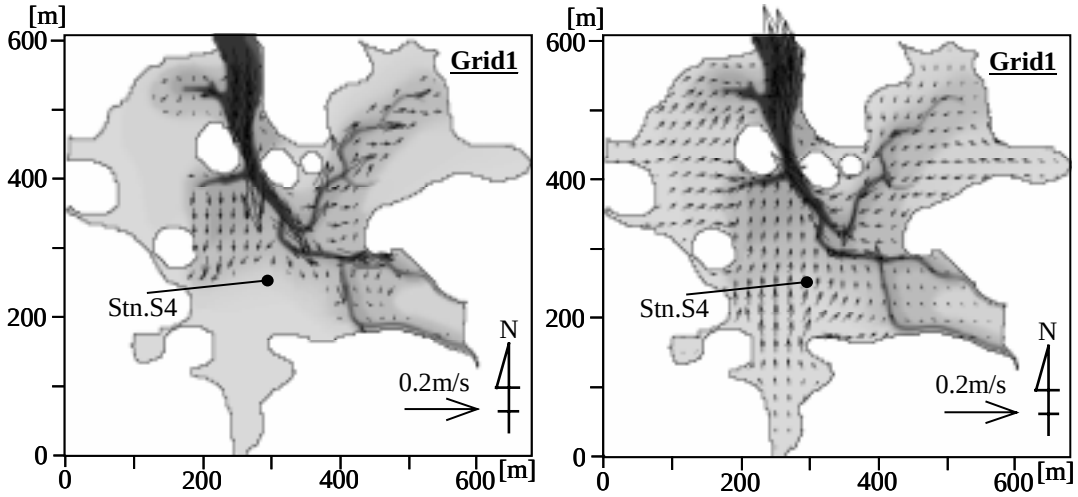

(a) Flood tide (Aug. 16, 16:00) **(b)** Ebb tide (Aug. 16, 20:20)

Fig. 3 Horizontal flow patterns in Grid 1.

al., 2002), we perform the current simulation for the period from 1pm on August 16 to 11am on August 17, 2001. There was no flood event through the inflow rivers into the mangrove area in this period, and then the effect of tide is only taken into account in the computation. For the tidal current simulation, we employ the observed data for the water elevation at the river mouth, placing on the northern open boundary in Grid 1, as depicted in **Fig. 2**. We use the bathymetry data in the computation as illustrated in **Fig. 1**.

Since there exists an exposed tidal flat in the computational region at low tides, in this computation, we need to treat a shoreline as a moving boundary. For the calculation of the

moving boundary, the dry and wet areas are decided with the water depth of which the threshold value is 0.10m.

3. Results and discussion

3.1 *Horizontal flow patterns in the swamp*

Figure 3 shows the horizontal flow patterns in Grid 1 at 16:00 and 20:20 on August 16, corresponding to the flood and ebb tides, respectively. In the figure, the velocity vectors are depicted only in the inundated area. While, at the flood tide, the seawater goes toward the interior of the swamp through the creek from the river mouth, the ebb current in the swamp mainly flows to the river mouth. These results indicate that the swamp current parallel to the surrounding creek appear appreciably in addition to the that normal to the creek, in which the latter is a well-known hydrodynamic phenomenon in swamps (e.g., Wolanski et al., 1992). It should be also noted that the velocity in the swamp is quite less than that in the creek due to the vegetation drag. To confirm the numerical performance in Grid 1, the observed and computed results for the water elevation and horizontal currents in the swamp (Stn.S4) are shown in **Fig. 4**. The comparison of the observed and computed results indicates that the computational results give acceptable agreements with the observed data.

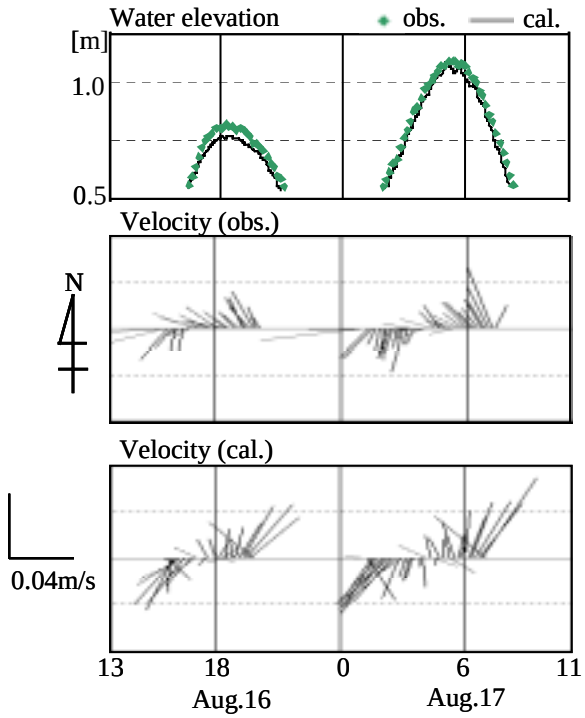

Fig. 4 Comparison of observed and computed results at Stn.S4 (Grid1).

3.2 *Flow structures in the creeks*

Figure 5 represents the computational results for the flow structures around the creeks, referred to here as Creeks A and B, in Grid 2 at the same flood and ebb tides as shown in **Fig.3**. The computational results in Grid 2 exhibit that the appreciable differences of the horizontal velocities in the creek are displayed in the computational results in Grid 2 although those are not clearly shown in the computational results in Grid1. At the flood tide, the creek current near the left bank of the swamp is noticeably larger than that near the right bank of the swamp in both the creeks. On the other hand, at the ebb tide, the peak values of the creek current appear near the right bank of the swamp. These variations of the creek current give qualitatively agreements with the observed results obtained by the authors (Nihei et al., 2002). These lateral distributions of the horizontal velocities in the creek may be formed due to morphological features of the meandering creeks and the influence of the larger-scale flow patterns in the mangrove swamp, as depicted in **Fig.3**.

Figure 6 indicates the time sequences of the observed and computed velocity in the parallel

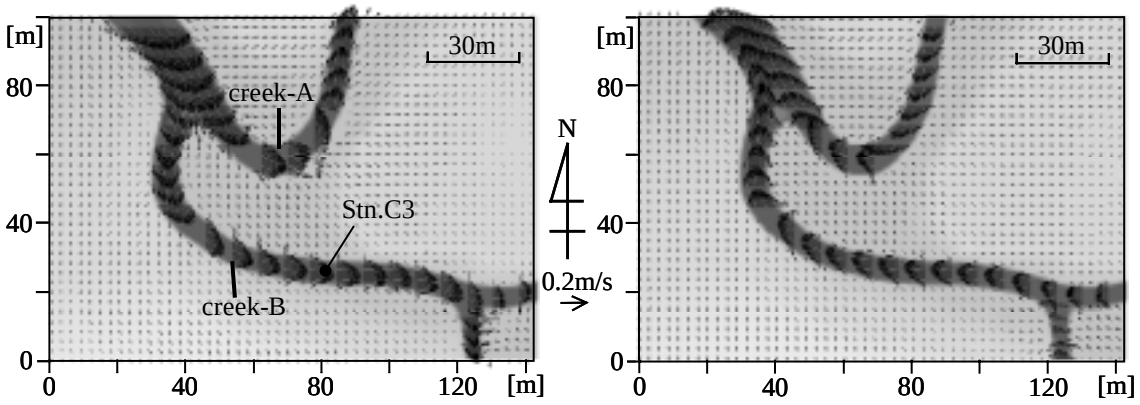

(a) Flood tide (Aug. 16, 16:00) **(b)** Ebb tide (Aug. 16, 20:20)

Fig. 5 Flow structures around the creeks in Grid 2.

direction to the creek B at Stn.C3. To check the fundamental performance of the nesting procedure in the computation, the computational results in Grid 1 and 2 are shown here. The comparison of these results illustrates that the computational results in Grid2 give better agreements with the observed data than those in Grid 1. The numerical accuracy for the creek currents becomes better with the increase of the gird resolution, and hence the nesting procedure used in the present study works well for the evolutions of the tidal current in the mangrove estuary.

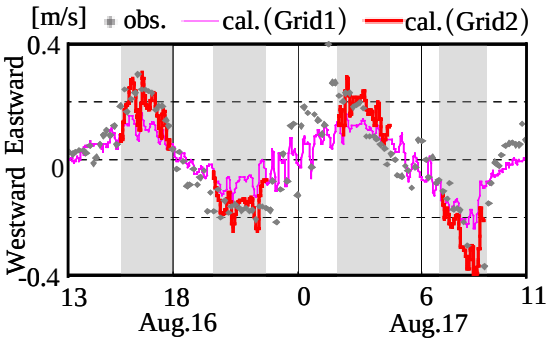

Fig. 6 Time sequences of the observed and computed creek velocity at Stn.C3.

3.3 *Horizontal large-eddy motion around the creek*

The computational results in Grid 3 with the grid resolution of 0.25m are indicated in **Fig. 7**, in which velocity vectors and contour of vorticity at the ebb tide (Aug. 16, 20:38) are depicted with the dashed line corresponding to the boundary between the creek and swamp. The results reveal that there appears a series of horizontal large-scale eddies near the boundary between the creek and the left bank of the swamp. It is also found that the evolution of the large eddies may be different near the left and right banks of the swamp and vary considerably in the flood and ebb tides. These large-eddy structures in the creek do not appear in Grid 1 and 2 with relatively lower grid resolutions. These facts demonstrate the fundamental applicability of the nesting procedure to the tidal current simulation in the mangrove area.

4. Conclusions

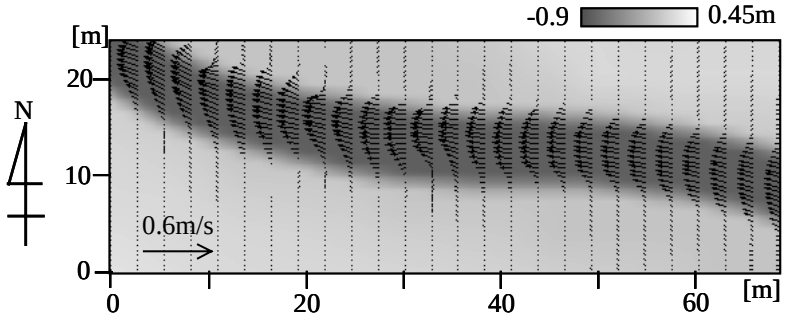

(a) Horizontal velocity vectors and bathymetry map

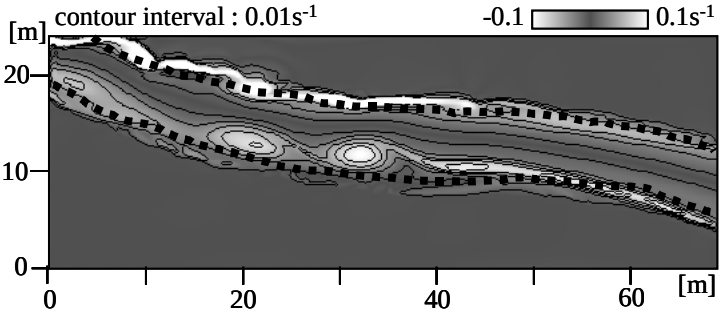

(b) Vorticity contour

Fig. 7 Horizontal large-eddy structures around the creek B at 20:38 on August 16 (ebb tide).

To efficiently perform the current simulation in a R-type mangal, we attempt to apply a nesting procedure to the computation of flow fields in the mangrove area at Fukido River estuarine section of the Ishigaki Island, Okinawa, Japan. In the computation, we adopt three computational domains with the different grid resolutions and domain sizes. The numerical accuracy of the creek velocity in Grid 2 with the relatively higher grid resolution becomes much better than that in Grid 1 with relatively the lower grid resolution, and hence we validate the nesting procedure used here for the tidal current simulation in the mangrove estuary. It should be also noted that the present numerical model can reproduce the lateral distribution of the creek velocity and the evolutions of the horizontal large-scale eddies around the creeks.

Acknowledgments

This study was partially supported by the Ministry of Education, Science, Sports and Culture, Grant-in-Aid for Scientific Research (B) (1) (no.12450198) and (C) (2) (no.13650573).

References

Lugo, A. E. and Snedaker, S. C. (1974). The ecology of mangroves, *Annual Review of Ecology and Systematics*, **5**, 39-64.

Mazda, Y., Kanazawa, N. and Wolanski, E. (1995). Tidal asymmetry in mangrove swamps,

Hydrobiologia, **295**, 51-58.
Nadaoka, K. and Yagi, H. (1998). Shallow-water turbulence modeling and horizontal large-eddy computation of river flow, *Journal of Hydraulic Engineering*, **124**, 5, 493-500.
Nihei, Y., Nadaoka, K., Kumano, R., Sato, K. and Machida, Y. (2001). A new multi-nesting approach for coastal ocean model, *Proc. of 11th PAMS/JECSS*, 365-368.
Nihei, Y., Yokoi, J., Aoki, Y., Tsunashima, Y., Sato, K. and Nadaoka, K. (2002). A field observation on 3D flow structure and turbulence characteristics around a mangrove creek, *Proc. of Coastal Engineering, JSCE*, **49**, 2, 1196-2000 (in Japanese).
Wolanski, E., Mazda Y. and Ridd, P. (1992). Mangrove hydrodynamics in Tropical mangrove ecosystems (eds. Robertson, A. I. and D. M. Alongi), *American Geophysical Union*, 43-62.